PCCP

Coherent D_2 rotational tunneling and incoherent D_2 dynamics in a solid non-classical RuD_2 complex studied by ^2H solid state NMR spectroscopy

Frank Wehrmann,[a] Tina P. Fong,[b] Robert H. Morris,[b] Hans-Heinrich Limbach[a] and Gerd Buntkowsky*[a]

[a] *Institut für Chemie der Freien Universität Berlin, Takustrasse 3, D-14195 Berlin, Germany*
[b] *Department of Chemistry, University of Toronto, 80 St. George Street, Toronto, Ontario, Canada M5S 3H6*

Received 24th May 1999, Accepted 12th July 1999

The ^2H solid state NMR spectra and T_1 relaxation data of a transition metal η^2-dideuterium complex, namely *trans*-$[Ru(D_2)Cl(PPh_2CH_2CH_2PPh_2)_2]PF_6$, have been measured in the temperature regime from 5.4 to 320 K. In the $Ru–D_2$ sample, coherent and incoherent exchange processes on the time scale of the quadrupolar interaction have been found, leading at low temperatures to a tunnel splitting of the ^2H NMR spectrum. With increasing temperature a slight increase of the tunnel splitting is observed, in conjunction with a strong increase of the incoherent exchange process, which finally, at temperatures above 20 K, destroys the tunnel splitting and determines the spectral line shape. For the description of the experimental spectra a Liouville formulation of the Alexander–Binsch NMR line shape theory, adapted for exchanging deuterons, is employed. It is shown that the whole evaluation of the ^2H magnetization takes place in four 2D and two 4D subspaces of the 81D Liouville space, leading to a drastic simplification of the numerical efforts in the simulation of the spectral line shapes. The height of the tunnel barrier calculated from the value of the tunnel splitting is 270 meV (6.22 kcal mol^{-1}). The incoherent exchange rates extracted from the spectra and from T_1 relaxation data are analyzed in terms of a Bell tunneling model, with a temperature dependent effective potential.

Introduction

The structure and dynamics of transition metal hydride complexes with non-classical structures, that is, with one or more η^2-bound dihydrogen ligands, is a matter of current experimental and theoretical interest. Following the pioneering work of Kubas *et al.*[1,2] a whole series of transition metal polyhydrides with hydrogen distances varying between 0.8 and 1.7 Å has been synthesized.[3–8] These η^2-bonded transition metal dihydrides can be considered as model compounds for short lived intermediate steps in catalysis[9] (Fig. 1). In these compounds the hydrogen atoms are not fixed in space, as in conventional hydrogen bonds, but exhibit a rather high mobility. In particular, they can exchange their positions. The mutual exchange of the hydrons can be regarded as a hindered 180° rotation around the axis intersecting the $M–H_2$ angle.[10–12]

The rotational barrier is caused mainly by the chemical structure from the binding to the metal and sometimes also by crystal effects from neighboring molecules. The two-fold symmetry of the barrier causes a splitting of the energy eigenstates into states with even and odd symmetry (see Fig. 2). For identical hydrogen isotopes, the quantum mechanical symmetry principles have to be fulfilled, leading for spin M particles to the formation of *para*-states with antiparallel and *ortho*-states with parallel nuclear spins. The height of the barrier determines the energy difference between the lowest even and odd symmetry, the so called tunnel splitting, which can be expressed as a tunnel frequency ν_t. This tunnel splitting depends very strongly on the hindering potential, varying from 10^{12} Hz for dihydrogen gas to a few Hz as the depth of the potential is increased. Due to this large range of tunnel frequencies no single spectroscopic technique is able to cover the whole dynamic range. While fast coherent tunneling in the frequency range of GHz to THz has been studied by incoherent neutron scattering (INS),[13,14] relatively slow tunneling processes in the frequency range of Hz to kHz have been investigated by ^1H liquid state NMR spectroscopy (for example ref. 14–21 and many others). In these ^1H liquid state NMR studies the tunnel frequency is usually termed "quantum exchange coupling", due to the fact that the effect of the tunneling on the ^1H liquid state NMR spectra is equivalent to the effect of an indirect spin coupling (*J* coupling).

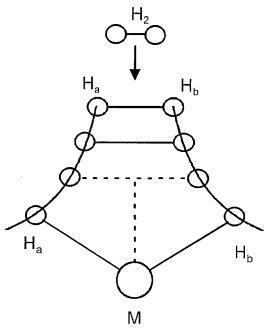

Fig. 1 Sketch of a hydrogen molecule binding to a transition metal. When the H_2 or D_2 molecule becomes bound to a transition metal, different states are passed, ranging from the free hydrogen molecule over various dihydrogen states to the strongly bound dihydride. These states can be characterized by their R_{HH} or R_{MH} distance as reaction coordinate. The depth of the rotational potential $V(R_{HH}, R_{MH}, \phi)$ will depend strongly on the reaction coordinate, resulting in tunnel splittings (energy differences between the lowest energy states) in the range from 0 to 10^{12} Hz.

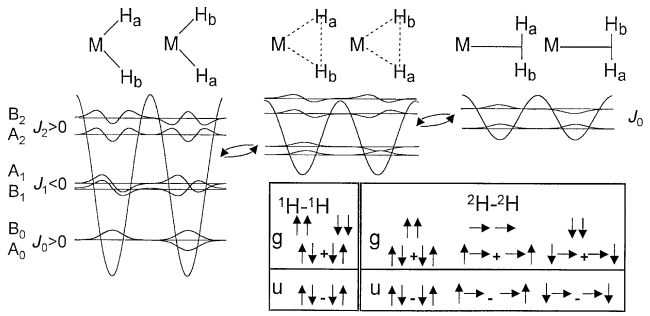

Fig. 2 Sketch of the energy eigenstates of a dihydrogen H_a–H_b system in a twofold rotational potential and symbolic representation of the symmetry adapted spin eigenfunctions. The spatial eigenstates are labeled $\mathbf{A}_k$ and $\mathbf{B}_k$, according to the irreducible representation of the C_2 group. The spin functions are labeled as **g** (*gerade*) for the even and **u** (*ungerade*) for the odd linear combinations. The tunnel splitting is the energy difference between adjacent levels $J_k = E(\mathbf{B}_k) - E(\mathbf{A}_k)$. For a pair of identical hydrogen isotopes the whole wave function has to be either antisymmetric (^{1}H–^{1}H, fermionic system) or symmetric (^{2}H–^{2}H, bosonic system). Thus for an ^{1}H–^{1}H pair, the spatial $\mathbf{A}_k$ functions couple to the **u** and the $\mathbf{B}_k$ to the **g** spin functions and for an ^{2}H–^{2}H pair, the spatial $\mathbf{A}_k$ functions couple to the **g** the $\mathbf{B}_k$ to the **u** spin functions.

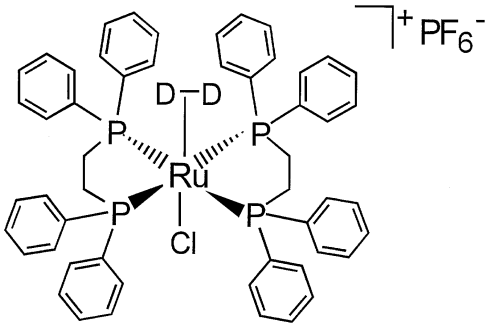

Fig. 3 Structure of the Ru–D_2 complex, *trans*-$[Ru(D_2)Cl(PPh_2CH_2CH_2PPh_2)_2]^+PF_6^-$.

In between the dynamic ranges of INS and ^{1}H liquid state a large dynamic gap is left in spectroscopic studies of coherent tunneling. In principle it would be possible to close a part of this gap by ^{1}H solid state NMR spectroscopy. However, ^{1}H NMR is mainly suited for the study of liquid samples, due to the following reasons: (i) in the solid state the strong magnetic dipolar interaction will in general couple the interesting protons to neighboring bulk protons, which will destroy the necessary spectral resolution to observe the tunneling of the protons; (ii) even if the tunneling spin pair is well separated from other protons it is difficult to observe the tunnel processes, since the dipolar interaction between these protons, which dominates the spectrum, is not influenced by the tunneling.

In a recent publication[22] we have proposed the use of ^{2}H solid state NMR spectroscopy to close a part of this dynamic gap. Deuterons are quadrupolar nuclei, which exhibit strong electric quadrupolar interactions, which are typically on the order of 100 kHz.[23] For non-oriented samples the quadrupolar interaction gives rise to the well-known line shape features in solid state ^{2}H NMR spectra. The quadrupolar interaction reflects the symmetry of the electric field gradient tensor at the position of the nucleus studied and is a very efficient measure of its electronic binding characteristics. Changes in the orientation of the quadrupolar tensor with respect to the external magnetic field are a very sensitive probe for any type of nuclear motion inside the sample. Due to this fact, besides numerous studies of incoherent motions (see for example the text book by Schmidt-Rohr *et al.*[24]), there are also several studies where coherent ^{2}H motions have been observed in methyl groups[25–29] and in fact methyl group tunneling seems to be quite a common phenomenon at low temperatures.[30] In solid dideuterium systems, however, until now, no experimental evidence had been found for coherent tunneling, mainly because finding a suitable system for the study of tunneling by ^{2}H NMR is no trivial task, because not only the height of the rotational barrier must be in the right range, but it is also necessary that a stable selective deuteration of the η^2-bound hydrogen positions can be achieved.

The complex *trans*-$[Ru(D_2)Cl(dppe)_2]PF_6$ (dppe = $PPh_2CH_2CH_2PPh_2$; see Fig. 3) was chosen for study for several reasons. Most importantly it can be prepared in a pure isotopic state from D_2 gas under controlled conditions without the formation of other species containing Ru–D or C–D bonds. Experience has shown that deuteration of many other complexes leads to unwanted deuterium incorporation into C–H bonds of the ligands of the dideuterium complex. Other advantages are the high stability of the complex in the solid state and the low cost of synthesis. One disadvantage is that single crystal neutron diffraction has not yet been applied to determine the H–H distance of the dihydrogen complex. The single crystal X-ray diffraction study at room temperature did not allow the precise location of the hydrons.[31]

However, the H–D coupling constant of the η^2-HD complex in solution, as determined by ^{1}H NMR spectroscopy, can be used to estimate an H–H distance of 0.99 Å.[8] This distance is somewhat longer than the short H–H distances of about 0.85–0.90 Å observed for dihydrogen complexes with strong H–H bonding. This elongation of the ^{2}H–^{2}H ligand of our Ru complex may be an important factor in the successful observation of the deuterium tunneling phenomenon. Short dihydrogen ligands display hydrogen tunneling at very high frequencies (3–30 cm^{-1}) that are detected by inelastic neutron scattering;[13,14] the corresponding tunneling in short dideuterium ligands would also be expected to occur at frequencies above the ^{2}H NMR scale (kHz). The frequency of tunneling of deuteria in dideuteride complexes (typical ^{2}H···^{2}H distances of greater than 1.6 Å) would be expected at very low frequencies considering that H···H tunneling in these systems has been detected by ^{1}H NMR when the frequency is in the range 50–10 000 Hz.[5,32] Therefore to detect a ^{2}H tunneling in the kHz frequency range of ^{2}H NMR, a ^{2}H···^{2}H distance greater than 0.90 Å but much less than 1.6 Å is probably required.

This paper now presents, to the best of our knowledge for the first time, experimental evidence for the presence of coherent dihydrogen tunneling in a solid transition metal–D_2 complex. From these data the height of the corresponding energy barrier is estimated.

The rest of this paper is organized as follows. First, a brief discussion of coherent and incoherent tunneling processes and an introduction into the Alexander–Binsch formalism for describing the spectral exchange is given. Next follows a description of the numerical methods used for calculating the spectra and the experimental section. Finally, the experimental results are presented, discussed and summarized.

Theory

Coherent rotational tunneling

The basic principles of the coherent tunnel exchange can be most easily discussed using the model of a one-dimensional hindered quantum mechanical rotor. In this model it is assumed that the distance between the two hydrons, as well as their distance from the metal, does not change and only the angular position, described *via* an angle ϕ, is used as a degree of freedom.

The corresponding Schrödinger equation of a rigid rotor in a harmonic twofold potential is expressed as eqn. (1) ($2V_0$

describes the depth of the hindering potential):

$$-\frac{\hbar^2}{2mr^2}\frac{\mathrm{d}^2}{\mathrm{d}\varphi^2}\psi - V_0[1-\cos(2\varphi)]\psi = E\psi \qquad (1)$$

This is a Matthieu type of differential equation which has well known solutions with the following properties: due to the C_2 symmetry of the problem, the resulting eigenstates have either even or odd symmetry and the whole Hilbert space splits up into an odd and an even subspace. The corresponding eigenfunctions can be easily calculated numerically by expanding eqn. (1) into a matrix eigenvalue problem using for example appropriately normalized sine (for the odd subspace) and cosine functions (for the even subspace) as base functions. The resulting eigenfunctions in these two sets are cosine type functions, $C_n(\phi)$, which are a superposition of the cosine functions, and sine type functions, $S_n(\phi)$, which are a superposition of the sine functions (Fig. 4). The ground state is always a cosine type state with even symmetry and the first excited state is always a sine type function with odd symmetry. The energy differences between different C_n or S_n depends strongly on the depth of the potential $2V_0$ and varies between zero and the order of typical rotational μ-wave or IR transitions. At temperatures in the range of 10 K only the lowest pair of eigenstates is thermally populated. If both hydrons are identical (*i.e.* both are ^{1}H or ^{2}H) the Pauli exclusion principle has to be fulfilled.

From this it follows, that the spatial states are connected to spin states in such a way that the whole wave function is either antisymmetric (for ^{1}H) or symmetric (for ^{2}H). Due to this the energy difference ΔE between the lowest two spatial eigenstates can be seen as an exchange coupling J_0 in NMR spectroscopy, similar to the Dirac exchange interaction of electronic spins. As a result a spin tunnel hamiltonian which describes the splitting between adjacent states of different symmetry can be defined. If the tunnel splitting is of the magnitude of interactions in NMR spectrum it is directly visible in the NMR spectrum.

If several pairs of tunnel levels are thermally populated the thermal average of the different pairs of tunnel levels has to be calculated. As long as only a few levels far below the barrier are contributing, the various v_{ti} values will be small compared to the thermal exchange rates between the level pairs and the averaging can be done by summing up the individual values of v_{ti} times their thermal population, which can be approximated

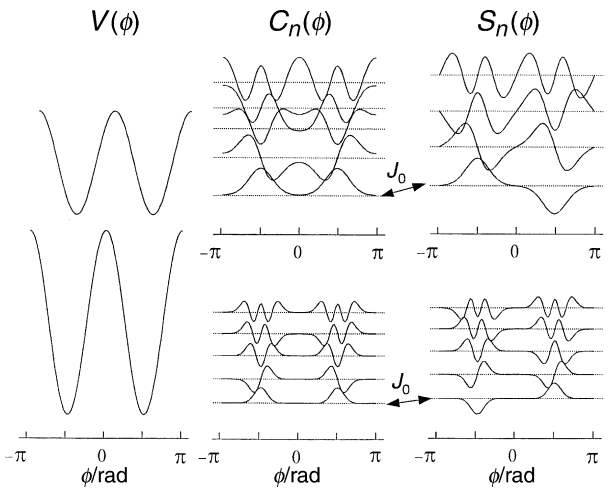

Fig. 4 Sketch of eigenstates and energy eigenvalues of the Schrödinger equation of a rigid D_2 rotor [eqn. (1)] in a harmonic twofold potential for two different depths of the potential barrier. Upper panel: $V_0 = 10 \times 10^6$ MHz, $J_0 = 6410$ MHz, lower panel: $V_0 = 100 \times 10^6$ MHz, $J_0 = 60$ Hz. Left: potential energy curve $V(\phi)$, middle panel: cosine type eigenfunctions $C_n(\phi)$, right panel: sine type eigenfunctions $S_n(\phi)$. The energy shift between cosine and sine functions has been increased artificially to demonstrate the differences in J_n.

using the population of one of the connected levels (v_{ti} = tunnel splitting between level pair i, k = Boltzmann constant, Z = partition function):

$$v_t = \frac{1}{Z}\sum_i v_{ti}\exp\left(-\frac{E_i}{kT}\right) \qquad (2)$$

The situation becomes more difficult if the values of v_{ti} are comparable or greater than the thermal population or decay rates. In this regime, a transition from coherent to incoherent exchange will take place, as described in ref. 14 in more detail.

Despite the large range of tunnel frequencies, varying between Hz and THz it is possible to describe the whole dynamic by a single theory:[14] Depending on the size of the tunnel frequency the two hydrons will exhibit strong differences in their dynamic behavior. For a low barrier height, a large tunnel frequency is observed. The dihydrogen pair will be at least partially delocalized and act more or less like a one-dimensional non-rigid quantum mechanical free rotor, similar to *para*-H_2 and *ortho*-H_2, allowing coherent (*i.e.* strictly periodic) exchange processes of the individual hydrons with the tunnel frequency v_t. For high potential barriers the tunnel splitting goes to zero, no coherent exchange processes take place and each hydron is fixed in one potential minimum. In this situation for an exchange of the two hydrogens a coupling to external degrees of freedom is necessary. In this scenario the exchange of the two hydrogens is describable as a thermally activated rate process. Compared to the previous coherent exchange, the thermally activated rate process corresponds to an incoherent exchange of the two hydrons, which leads to an exponential decaying curve for the probability of finding one hydron on its initial position.

NMR line shape theory

Due to the fact that the typical time scale for ^{1}H NMR line shape analysis is of the order of a few Hz to several kHz and the typical transition times of vibronic processes are of the order of typical IR frequencies, *i.e.* 10^{11} Hz, these processes can be treated separately from the spin degrees of freedom. The resulting theory for describing the NMR line shape of protons was developed by Alexander[33] and Binsch *et al.*[34,35] They describe the NMR line shape quantitatively in terms of a quantum mechanical density matrix formalism, where only the nuclear spin degrees of freedom are treated quantum mechanically and the spatial degrees of freedom (bath coordinates) are treated *via* phenomenological rate constants. Recently it was realized that the Alexander–Binsch formalism can also be employed to describe the simultaneous presence of coherent and incoherent exchange processes[14] in transition metal hydrides, modeling the complete nuclear motion *via* two phenomenological constants, a rate constant k describing the incoherent exchange and the coherent exchange splitting v_t. A theoretical interpretation of these rate constants has been given by Szymanski[36,37] and Scheurer *et al.*[32,38]

In the following we want to briefly summarize the NMR line shape theory of a system of two deuterons bound in a twofold potential and subject to coherent and incoherent exchange. A detailed discussion of this formalism can be found in ref. 22. To avoid confusion between the usual spin–spin coupling hamiltonian and the exchange interaction (which has a different hamiltonian), we will follow our previous paper[22] and use the letter X for the coherent exchange rate.

In a first approximation in the solid state we can restrict ourselves to consider only the leading interactions, *i.e.* the quadrupolar interaction and the coherent tunnel exchange:

$$\begin{aligned}\hat{H} &= \hat{H}_Q + \hat{H}_X \\ \hat{H}_Q &= q_1(\hat{I}_{z1}^2 - \tfrac{2}{3}) + q_2(\hat{I}_{z2}^2 - \tfrac{2}{3}) \\ \hat{H}_X &= X\hat{P}(\hat{\boldsymbol{I}}_1, \hat{\boldsymbol{I}}_2)\end{aligned} \qquad (3)$$

In these equations, q_1 and q_2 are the quadrupolar couplings of the spins, X is the coherent tunnel frequency, $\hat{P}(\hat{I}_1, \hat{I}_2)$ is the permutation operator of the two spins $\hat{I}_1$ and $\hat{I}_2$ in spin space.

In contrast to the coherent exchange interaction the quadrupolar interaction depends on the relative orientation of the magnetic field to the quadrupolar tensor. Since both deuterons can be assumed to be chemically equivalent, their quadrupolar tensors are related by a geometrical transformation. If we assume C_{2v} symmetry of the M–D_2 group by neglecting possible crystal effects, one of the three principal axes of the quadrupolar tensor will be perpendicular to the M–D_2 plane, and the axis bisecting the bond angle (2α) will be a twofold symmetry axis (C_2). A coordinate system (Fig. 5) is chosen in such a way that the z-axis bisects the bond angle and that the y-axis is perpendicular to the bond plane. The two quadrupolar tensors are related by a rotation $\boldsymbol{R}$ with angles $\pm\beta$ around the y-axis of the coordinate system. The angle β depends on the strength of the electric field gradients (EFG) caused by the metal and by the other deuterons. In particular, in the case of a dihydride, β will be half the bond angle (*i.e.* $\beta = \alpha$). For molecular dihydrogen with a very weak interaction with the metal or dihydrogen complexes where the M–D bonding is negligible compared to the D–D bonding, the two quadrupolar tensors will have their z-axis in the direction of the D–D axis, *i.e.* $\beta = \pi/2$. For simplicity we will call these complexes pure dihydrogen complexes.

The coherent tunnel exchange can be described by the permutation operator $\hat{P}(\hat{I}_1, \hat{I}_2)$ times the tunnel frequency X, *i.e.*:

$$\hat{H}_X = X_{12}\,\hat{P}(\hat{I}_1, \hat{I}_2) \tag{4}$$

In the product base of the two spins, the matrix representation of $\hat{P}(\hat{I}_1, \hat{I}_2)$ can be easily calculated from ($|\mu\nu\rangle$ = product base function):

$$\hat{P}(\hat{I}_1, \hat{I}_2)\,|\mu\nu\rangle = |\nu\mu\rangle \tag{5}$$

As long as no incoherent exchange processes are present in the sample the NMR signal (FID) is given as the expectation value of the $M_+ = \langle I_+ \rangle$ operator. Fourier transformation of this time signal gives the corresponding spectrum. In non-oriented powder samples this spectrum is a function of the orientation, which can be described by the polar angle β and the azimuth angle α. So finally, the NMR spectrum is given as the integral over all orientations, *i.e.*:

$$M_+(\nu) = \int_0^{2\pi} \int_0^{\pi} M_+(\nu, \alpha, \beta) \sin\beta \, \mathrm{d}\beta \, \mathrm{d}\alpha \tag{6}$$

In the absence of incoherent exchange processes, the whole dynamics of the system can be described directly in the Hilbert space of $\hat{H}$, and thus the spectra can be calculated directly from $\hat{H}$. However, as soon as incoherent exchange mechanisms are present, this approach is no longer valid. A method for tackling this type of problems is the Alexander–Binsch formalism. The essence is that the whole kinetics of the M–D_2 system can be described by two empirical constants, the incoherent exchange constant k and the coherent tunnel exchange constant X. In general these two constants represent the thermal average of the tunnel splitting and the exchange constants, respectively, of the populated levels and thus will exhibit a nontrivial temperature dependence ($p_\xi(T)$ is the thermal population of level ξ):

$$k(T) = \sum_\xi p_\xi(T) k_\xi \tag{7}$$

$$X(T) = \sum_\xi p_\xi(T) X_\xi$$

In the Alexander–Binsch formalism the Liouville–von Neumann equation of the system density matrix has to be solved:

$$\frac{\mathrm{d}}{\mathrm{d}t}\,|\rho) = :-\hat{M}\,|\rho - \rho_\infty) \tag{8}$$

$\hat{M}$ is the temperature dependent dynamic superoperator, which describes relaxation ($\hat{R}$) coherent ($\hat{L}$) and incoherent ($\hat{K}$) dynamics: $\hat{M} = \hat{K} + \hat{R} + i\hat{L}$.

The formal solution of this equation is:

$$|\rho(t)) = \exp(-\hat{M}t)\,|\rho(0) - \rho_\infty) + |\rho_\infty) \tag{9}$$

From this solution the expectation values of the magnetization and thus the spectra for one orientation can be calculated and by integrating over all orientations the temperature dependent powder spectra are obtained. It should be noted that the principal difference between a coherent and an incoherent exchange is that the coherent exchange will, in general, lead to a shift of the energy levels and thus to a splitting of the transition frequencies, while the incoherent exchange will cause a line broadening or line coalescence of the transition frequencies. Moreover, to influence the spectra there must be a difference in the relative orientations of the quadrupolar tensors, *i.e.* $2\beta \neq 0^0$. In particular for powder spectra the effect is most pronounced for $2\beta = 90^0$.

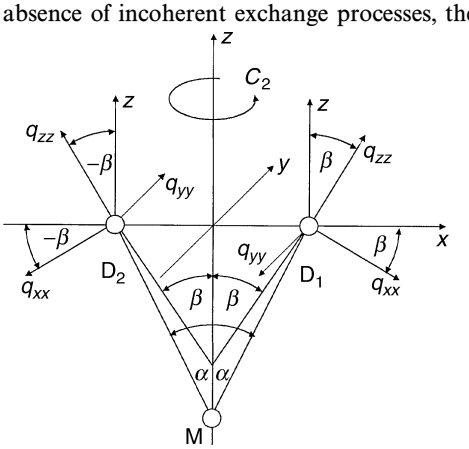

Fig. 5 Coordinate system used for describing the relative spatial orientation of the two quadrupolar tensors of deuterons D_1 and D_2. C_{2v} symmetry is assumed for the deuterons and therefore one of the principal axes (q_{yy}) is parallel to y. The quadrupolar tensor of deuteron 2 is obtained by a 180° rotation around the z-axis of the coordinate system. For describing the relative orientations of the tensors it is more convenient to use the angle between the z-axis and the q_{zz}-component. Note that in general the bond angle 2α will not coincide with the jump angle 2β, *i.e.* $2\alpha \neq 2\beta$.

Numerical methods and data evaluation

The nine Zeeman product functions of the two spin system were chosen as base functions for the matrix representation of the hamiltonians and the spectra were calculated for the initial condition of a 90^0 pulse applied to the spin system in thermal equilibrium. Effects of the finite pulse power and the spin echo experiment were taken into account using the formula given in ref. 24. The powder averages were calculated by integrating over a grid of 128 × 128 equally spaced polar angles φ and ϑ. In a first step the quadrupolar and coherent exchange couplings were determined by fitting the low temperature spectrum using a Hilbert space expression of the powder spectrum and neglecting incoherent exchange processes. In the next step the high temperature spectrum was fitted, assuming complete averaging of the two tensors. From this spectrum the angle between the principal axis systems (PAS) systems of the two quadrupolar tensors is determined.

These data were used for calculating the effects of the incoherent exchange in the following way. The 81 Liouville space base functions of the Liouville space were constructed and the Liouville, exchange and relaxation operators were expressed in these base functions and combined to the dynamic superoperator $\hat{M}$. From the representation of $|F_+)$ in the complete Liouville space the corresponding $|F_{+k})$ operators in the subspaces L_k were determined (see below in the results section)

and the spectra were calculated by diagonalization of the $\hat{M}_k$ operators transforming the $|F_{+k})$ operators into the eigenbase of $\hat{M}_k$. Again the grid of 128×128 equally spaced polar angles was employed for calculating the powder averages.

In the calculations, we started with the initial condition that a 90^0 pulse was applied to the spin system in thermal equilibrium and thus the initial density matrix $|\rho(0))$ is given by $|F_x)$:

$$|\rho(0)) = |F_x) = |I_{x1} + I_{x2}) \tag{10}$$

Spin lattice relaxation. Besides affecting the shape of the ^{2}H NMR spectra, coherent and incoherent exchange effects can also influence the ^{2}H spin lattice relaxation rates. Assuming that mainly the incoherent exchange will contribute to the spin lattice relaxation rate, in particular at higher temperatures, there is a direct relation between the characteristic time constant τ_c in the spectral density functions in the relaxation model and the incoherent exchange rates k_{12}:

$$\tau_c(T) = \frac{1}{2k_{12}(T)} \tag{11}$$

The actual spin lattice relaxation rate depends on the motional model of the exchange process. Several special types of motions are discussed in the literature namely: (a) isotropic rotational diffusion [eqn. (12b)[23]], (b) jump motions of the deuterons employing the model of ref. 39 and 40 (note: eqn. (12c) is calculated from the single crystal value given in ref. 40 by integrating the relaxation over all possible crystal orientations), (c) axial symmetric rotational diffusion[23]. In the general case, where the motional model is not known exactly, an effective coupling rate constant K^{EFG} can be used [eqn. (12a)].[41]

If $J(\tau)$ describes the spectral density function of the fluctuations, τ, respectively, τ_0, τ_1, τ_2, describe the isotropic or anisotropic correlation times and β the angle between rotation axis and tensor axis, respectively, the angle between the two tensor axes, the corresponding relaxation functions are (q_{cc} = quadrupole coupling constant):

$$\text{a} \qquad \frac{1}{T_1} = K^{EFG} J(\tau)$$

$$\text{b} \qquad \frac{1}{T_1} = 0.3\pi^2 q_{cc}^2 J(\tau)$$

$$\text{c} \qquad \frac{1}{T_1} = \frac{9}{160} \sin^2 \beta q_{cc}^2 J(\tau)$$

$$\text{d} \qquad \frac{1}{T_1} = 0.3\pi^2 q_{cc}^2 [\tfrac{1}{4}(\cos^2 \beta - 1) J(\tau_0) + 3 \sin^2 \beta \cos^2 \beta J(\tau_1) + \tfrac{3}{4} \sin^4 \beta J(\tau_2)] \tag{12}$$

The overall difference of the relaxation curves calculated with these models are relatively small on the large temperature range considered in this work (ω_0 = Larmor frequency).

$$J(\tau) = \left[\frac{\tau}{1 + (\omega_0 \tau)^2} + \frac{4\tau}{1 + (2\omega_0 \tau)^2} \right] \tag{13}$$

For the usual spectral density function [eqn. (13)] and an Arrhenius dependence of τ on the temperature a single T_1 minimum and a parabolic growth of T_1 as a function of the temperature is expected. The situation changes if τ exhibits a non-Arrhenius behavior, for example, due to tunneling. In this situation eqn. (11) can to be used to determine the exchange rates from the T_1 rates, if the position and value of the T_1 minimum is known.

Experimental section

The spectrometer

A detailed discussion of our home-built three-channel NMR spectrometer has been given recently.[42] Here only some salient features are reproduced. All experiments were performed at a field of 6.98 T, corresponding to a ^{2}H resonance frequency of 45.7 MHz on a standard Oxford wide bore magnet (89 mm) equipped with a room temperature shim unit.

For the ^{2}H channel a 2 kW class AB amplifier from AMT equipped with RF blanking for suppressing the noise during data acquisition was employed. All experiments were performed using a home-built 5 mm ^{2}H NMR probe. The probe is placed in a dynamic Oxford CF1200 helium flow cryostat. The sample temperature was controlled employing an Oxford ITC 503 temperature controller. During cooling, and before and after data acquisition, the sample temperature was controlled directly *via* a CGR-1-1000 sensor placed in the direct vicinity of the sample. This temperature was used to calibrate the readings of a second CGR-1-1000 sensor, which is part of the cryostat. During data acquisition, the first sensor was disconnected from the ITC 503 and grounded to protect the ITC from the RF and to avoid distortions of the signal. The RF was fed through a crossed diode duplexer, connected to the detection preamplifier and through the filters into the probe. Typical 90^0 pulse width was 3.0 μs, corresponding to 83 kHz $\boldsymbol{B}_1$ field in frequency units. All spectra were recorded using the solid echo technique, with an echo spacing of 30 μs. The repetition time of the experiments was between 10 and 60 s, depending on the T_1 relaxation time of the sample and the typical number of accumulations was 1600 scans per spectrum.

Samples and preparation

Under Ar, 2.0 g (1.8 mmol) of $[RuCl(dppe)_2]PF_6$ (ref. 43) was dissolved in 30 mL CH_2Cl_2. The resulting red solution was cooled to $-25\,^{\circ}C$ (monitored with a thermometer) using a dry ice/acetone bath. Deuterium gas was bubbled into the solution until the color changed to yellow (approx. 5 min). Then Ar was immediately purged through the system to remove the excess deuterium gas. Diethyl ether (100 mL) that had been precooled to $-25\,^{\circ}C$ was quickly added to precipitate the product. When the precipitate settled, the ether was syringed out and the cream colored product was dried under a stream of Ar. In a glove bag filled with Ar, *trans*-$[Ru(D_2)Cl(dppe)_2]PF_6$ was tightly packed into a 5 mm NMR tube up to a level of 25 mm and then glass wool was added. The tube was placed under vacuum and flame-sealed just above the glass wool.

^{2}H NMR (CH_2Cl_2, 253 K): −12.4 ppm (s). When the sample was warmed to 293 K or if the sample was prepared at room temperature, the ^{2}H NMR also revealed resonances at 7.3 and 1.5 ppm caused by D–H exchange between the Ru–D_2 and C–H sites.

Results

Subspace structure of the Liouville space

One major problem in the simulation of the influence of the incoherent exchange rates on the ^{2}H NMR spectra is that, due to the size of the Liouville operator, the necessary numerical simulation of the spectra is very time consuming and renders it impossible to fit experimental spectra in a reasonable time. In a previous work[22] we tried to solve this problem by sorting the base functions of the Liouville space according to their multiple quantum orders, which led to a blocking of the superoperator $\hat{M}$. However, while this approach allowed the calculation of a spectrum with good resolution typically

within 3 h of CPU time, which is sufficient for simulations, for a real fit of experimental spectra a much faster calculation of the spectra is necessary. Realizing that the matrix representation of the $\hat{M}$ superoperator is highly sparse, we started to analyze the subspace structure of the Liouville space assuming the given initial condition of eqn. (10). We found that $\hat{M}$ can be transferred into a block diagonal form, where all the evolution of the measurable magnetization takes place in four two-dimensional and two four-dimensional subspaces L_k of the Liouville space. The resulting two-dimensional subspaces and suboperators $\hat{\hat{M}}_k$ are:

$$\hat{\hat{M}}_1 = \begin{bmatrix} -k + 2\pi i(q_1 + X) & k - 2\pi iX \\ k - 2\pi iX & -k + 2\pi i(q_2 + X) \end{bmatrix} \qquad L_1 = \begin{matrix} |0 - - -) \\ |-0 - -) \end{matrix}$$

$$\hat{\hat{M}}_2 = \begin{bmatrix} -k + 2\pi i(-q_1 + X) & k - 2\pi iX \\ k - 2\pi iX & -k + 2\pi i(-q_2 + X) \end{bmatrix} \qquad L_2 = \frac{|+\,0\,00)}{|0 + 00)}$$

$$\hat{\hat{M}}_3 = \begin{bmatrix} -k + 2\pi i(q_1 - X) & k + 2\pi iX \\ k + 2\pi iX & -k + 2\pi i(q_2 - X) \end{bmatrix} \qquad L_3 = \begin{matrix} |00 - 0) \\ |00\,0 -) \end{matrix}$$

$$\hat{\hat{M}}_6 = \begin{bmatrix} -k - 2\pi i(q_1 + X) & k + 2\pi iX \\ k + 2\pi iX & -k - 2\pi i(q_2 + X) \end{bmatrix} \qquad L_6 = \begin{matrix} |+\,+\,0+) \\ |+\,+\,+\,0) \end{matrix} \quad (14)$$

and the four-dimensional subspaces and suboperators are:

$$\hat{\hat{M}}_4 = \begin{bmatrix} -k - 2\pi iq_1 & 2\pi iX & -2\pi iX & k \\ 2\pi iX & -k - 2\pi iq_2 & k & -2\pi iX \\ -2\pi iX & k & -k - 2\pi iq_1 & 2\pi iX \\ k & -2\pi iX & 2\pi iX & -k - 2\pi iq_2 \end{bmatrix} \qquad L_4 = \begin{matrix} |-\,+0-) \\ |-\,+\,-0) \\ |+\,-0-) \\ |+\,-\,-0) \end{matrix}$$

$$\hat{\hat{M}}_5 = \begin{bmatrix} -k + 2\pi iq_1 & -2\pi iX & 2\pi iX & k \\ -2\pi iX & -k + 2\pi iq_2 & k & 2\pi iX \\ 2\pi iX & k & -k + 2\pi iq_1 & -2\pi iX \\ k & 2\pi iX & -2\pi iX & -k + 2\pi iq_2 \end{bmatrix} \qquad L_5 = \begin{matrix} |0+\,+\,-) \\ |+0+\,-) \\ |0+\,-\,+) \\ |+0-\,+) \end{matrix} \quad (15)$$

Experimental results

In the following the experimental results on the Ru–D_2 sample are presented. The experimental difficulty in these experiments stemmed mainly from a sensitivity problem caused by the low deuterium abundance in the sample due to the high molecular weight of the compound.

Fig. 6 compares experimental and simulated ^{2}H NMR spectra of the Ru–D_2 complex. In the temperature range between 20 and 230 K the ^{2}H NMR line corresponds to a typical ^{2}H NMR quadrupolar pattern with an asymmetry of $\eta = 0.2$. The width of the line decreases slowly with increasing temperature. At temperatures above 320 K an additional narrow component appears in the center of the spectrum.

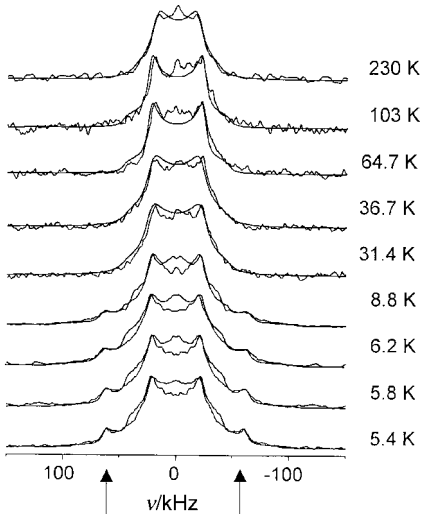

Fig. 6 Experimental and simulated ^{2}H NMR spectra of the Ru–D_2 complex, measured in the temperature range from 5.4 to 230 K. At temperatures below 8.8 K a splitting in the ^{2}H NMR line shape is clearly visible (arrows). This splitting can be explained by a coherent tunneling of the two deuterons in the Ru–D_2 sample. The simulations were performed with $q_{zz} = 80 \pm 3$ kHz (*i.e.* $q_{cc} = 107 \pm 4$ kHz), $\eta = 0$ and a jump angle between the two tensor orientations of $2\beta = 90°$.

This situation changes strongly in the temperature regime below 20 K. In this regime a strong increase of the spectral line width is observed, resulting in a spectrum at 5.4 K which has at the bottom approximately twice the width of the 320 K spectrum. Moreover satellite transitions appear with the singularities at frequencies of $\pm$ 60 kHz. The position of these singularities depends weakly on the temperature: a slight increase of the observed frequency with increasing temperature is found. The width of these singularities, which is rather narrow at 5.4 K, increases strongly with increasing temperature until they have disappeared at 22.8 K.

Fig. 7 displays the result of the T_1 measurements on the RuD_2 complex. Due to the low sensitivity of the sample we measured the spin lattice relaxation rates only at some selected temperatures. The lowest T_1 value (0.12 ± 0.02 s) was found at 97 K. At low temperatures the T_1 data show strong deviations from a simple Arrhenius behavior.

Discussion

A stable Ru complex, selectively labeled with D_2 in the η^2 bond, has been synthesized. The ^{2}H NMR spectra of this Ru–D_2 complex have been measured in the temperature range from 5.4 to 320 K. At temperatures below 20 K a splitting in

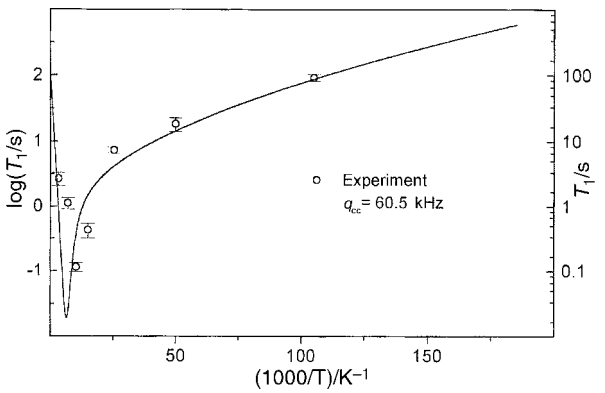

Fig. 7 T_1 relaxation data of the Ru–D_2 complex. Experimental points from line shape analysis and relaxation measurements. The solid line is calculated from the exchange rates calculated from the modified Bell model using the value of $K^{EFG} = 0.3\pi^2$ (60 kHz)^2.

the ^2H NMR spectra has been found, leading to satellite transitions at frequencies of ± 60 kHz. At higher temperatures these satellite transitions disappear and the ^2H NMR spectrum narrows.

In principle there are several possible explanations for the splitting observed at low temperatures, which are not necessarily mutual exclusive: a chemical impurity, which is not visible in the spectra at higher temperatures, for example due to very long T_1 relaxation times or because it is hidden in the more narrow line of the RuD_2; a type of phase or glass transition, where a fast motional process is freezing only for a part of the ^2H spins, resulting in the more broad component; chemical shielding and/or spin–spin coupling interactions; homonuclear dipolar interactions between the deuterons; heteronuclear dipolar interactions between the deuterons and the Ru nucleus; heteronuclear dipolar interactions between the deuterons and other surrounding nuclei, for example ^1H or ^{31}P nuclei; the proposed quantum mechanical exchange mechanism.

Assuming that the observed splittings in the 5.4 K spectrum are the Pake singularities of a second spectrum, which is caused by an impurity in the sample, the concentration of this impurity can be estimated as *ca.* 40% of the whole deuterium concentration, which can be excluded, due to the careful preparation of the sample and due to the low temperatures where the lines appear. In principle, a phase transition would be possible to account for the appearance of two distinct spectra. However, the very low activation energy of this transition and the fact that at the regime below 20 K the intensity ratio of the broader and the more narrow components does not change, makes such an explanation relatively improbable.

Thus we conclude that the lines have to be attributed to the deuterons in the RuD_2 complex. Typical ^2H chemical shielding interactions are of the order of 20 ppm and below, corresponding to about 1 kHz at 7 T for ^2H spins and typical ^2H–^2H spin–spin interactions are of the order of few Hz, which are both much too low to explain the observed splitting. The effect of homonuclear dipolar interactions on the spectral line shape can be estimated by simulation of the corresponding spectra. The result of these simulations (not shown) is, that ^2H–^2H dipolar couplings of approximately 15–20 kHz, corresponding to a $^2H\cdots{}^2H$ distance of 0.5 to 0.6 Å, would be necessary to explain the observed splitting. Spectra calculated with these values give only a very bad reproduction of the experimental spectra and the calculated $^2H\cdots{}^2H$ distances are much too low and not reasonable on the basis of the expected distance of about 1.0 Å (see the Introduction); thus such an explanation can be excluded. Heteronuclear interactions between the deuterons and the Ru nucleus can also be excluded since, due to the low gyromagnetic ratio of the NMR active ruthenium isotopes, Ru–D distances, *i.e.* bond length, in the range of 0.3 to 0.4 Å are necessary to explain a dipolar splitting of 20 kHz. A similar argument is valid for dipolar couplings to neighboring ^1H or ^{31}P nuclei. A calculation of the necessary distance range compatible with a splitting of 20 kHz yields $R_{max} = 1$ Å for ^1H and $R_{max} = 0.75$ Å for ^{31}P, respectively. Since such close distances can be excluded in the Ru–D_2 system one can exclude dipolar interactions as the origin of the low temperature and we conclude that the splitting has to be attributed to the proposed quantum mechanical exchange interaction.

Using this model the experimental spectra were simulated assuming a superposition of a coherent and an incoherent exchange process. From this model the following data are extracted: the angle between the tensor orientations, the coherent tunnel rate X_{12} and the incoherent exchange rate k_{12}. The coherent tunnel rate X_{12} varies only weakly and the incoherent exchange rate k_{12} varies strongly as a function of the temperature. With the exception of the weak narrow central component in the 230 K spectrum, which accounts for approximately 3% of the spectral intensity, they give a good reproduction of all experimental spectra. Therefore we conclude that the weak narrow component is an experimental artifact and not related to the D_2 motion. In principle there are two different possible origins for this artifact, which are not necessarily mutually exclusive: the central line can be caused by an impurity in the sample, which is frozen at low temperatures and becomes liquid or gaseous at high temperatures, thus having a narrow and good visible line at high temperatures, while being invisible in the spectra at lower temperatures, due to its low intensity; an alternative explanation is that it stems from natural abundance deuterons in the phenyl rings. The X-ray structure analysis of the compound has shown that two of the phenyl rings become highly mobile at higher temperatures[31] and the amount of natural abundance deuterium in the phenyl ring is only one order of magnitude lower than the amount of deuterium in the labeled D_2 group.

The quadrupolar coupling and the angle between the principal axes of the two quadrupolar tensors were adapted from the simulations of the low temperature spectrum at 5.4 K and the high temperature spectrum at 320 K, assuming that the latter corresponds to the fast exchange limit. The best fit was obtained using an angle of $2\beta = 90 \pm 10°$ between the principal axis systems (PAS) and a nearly axial symmetric ($\eta < 0.1$) quadrupolar tensor with $q_{zz} = 80 \pm 3$ kHz.

Comparing this $90 \pm 10°$ angle with the bond angle of 34°, calculated from the estimated Ru–D distance of 1.7 Å and the D–D distance of 1 Å, it is evident that these angles do not coincide. The reason for this difference is shown in Fig. 8, which sketches the electron density distribution of the binding electrons for different dihydrogen systems. The left scheme corresponds to the usual situation of a simple dihydride with covalent bonds to the metal. In this situation the main electron density is distributed between the metal and the deuterons and thus the unique principal axis of the quadrupolar tensor will point in the bond direction, leading to a jump angle equal to the bond angle. The right scheme of Fig. 8 on the other hand shows the other extreme, *i.e.* a pure dihydrogen state, where the two hydrons are covalently bound and the unique axis of the quadrupolar tensors will point into the direction of the D–D bond, leading to a jump angle of 180°. The η^2-D_2 bond however corresponds to the intermediate case, where electron density is distributed in the whole M–D_2 system. In this situation in general none of the bond directions will be a principal axis of the quadrupolar tensors, resulting in a jump angle which is in between the bond angle and 180°, as in our case.

Fig. 9 shows an Arrhenius plot of the temperature dependence of X_{12} and k_{12}. A strong temperature dependence is observed for k_{12} while there is a very weak dependence for X_{12}. The temperature dependence of X_{12} is nearly linear in the temperature window between 5 and 20 K and can be fitted as (dashed line):

$$X_{12} = 26.7\ [\mathrm{kHz}] - 0.038\ [\mathrm{kHz \cdot K}] \cdot 1000/T \qquad (16)$$

Assuming the simple harmonic potential of eqn. (1) the height of the rotational barrier can be estimated. Using the

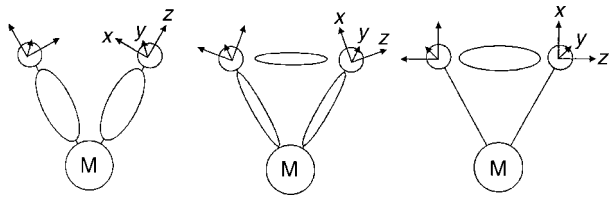

Fig. 8 Sketch of the orientations of the quadrupolar tensors for a dihydride (left), η^2-bond (center) and a dihydrogen complex (right). Detailed explanation is given in the text.

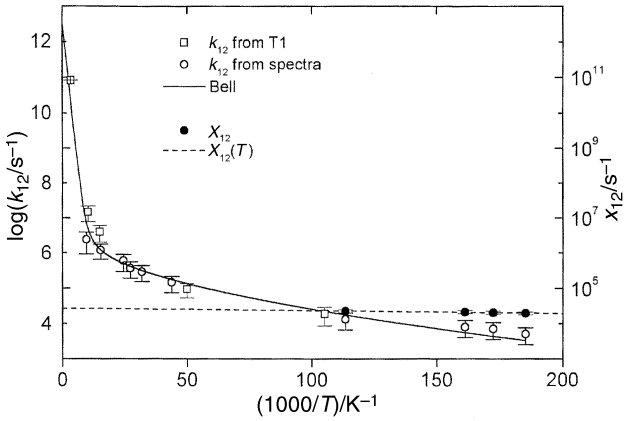

Fig. 9 Arrhenius plot of the temperature dependence of the coherent and incoherent exchange rates, extracted from Figs. 6 and 7. The solid line is the result of a fit of the temperature dependence of the incoherent rates using a modified Bell tunnel model (see text). The dashed line is a simple linear fit of the coherent tunnel rates.

value of $R_{HH} = 1$ Å, a rotational barrier of $2V_0 = 270$ meV (6.22 kcal mol^{-1}) is found.

The incoherent rates exhibit a much stronger temperature dependence, varying from 5 kHz at 5.4 K to *ca.* 2.5 MHz at 103 K. Above this temperature the exchange is so fast that it is not possible to extract further rates from the spectra. However, assuming that at low temperatures the exchange of the two deuterons is the only motion in the sample the ^{2}H T_1 relaxation should also be influenced by this motion and it should be possible to follow the exchange process by converting the T_1 rates to exchange rates. The resulting exchange rates, which were obtained for $K^{EFG} = 0.3\pi^2$ (60 kHz)^2 are also shown in Fig. 9.

The simulation of this temperature dependence was performed assuming a thermally activated tunneling process, described by a Bell type of tunneling. The high temperature rate in the tunnel model was chosen as 4×10^{12} s^{-1}.

In a first step a simple one-dimensional Bell tunneling model with a fixed D–D distance and constant height of the potential was employed. However this model leads to an unsatisfactory result, because the observed increase of k_{12} at low temperatures is not found in this model. Therefore we conclude that at least a two-dimensional model has to be employed for the description of the actual tunneling, where the average R_{HH} and/or R_{RuH} distances are functions of the temperature. To have a simple one-dimensional model for such a two-dimensional tunneling process, a temperature dependent effective tunnel barrier was employed, assuming that the effective potential as a function of the temperature can be described as a power law:

$$V_{eff}(T^{-1}) = V(T_0^{-1}) + [V(T_1^{-1}) - V(T_0^{-1})] \times \left(\frac{T^{-1} - T_0^{-1}}{T_1^{-1} - T_0^{-1}}\right)^G \quad (17)$$

The best fit of the experimental rates (solid line in Fig. 9) was found for an exponent of $G = 0.7$, *i.e.* for a relatively linear temperature variation of the effective potential, varying between 268 meV (6.18 kcal mol^{-1}) at 5.4 K and 129 meV (2.97 kcal mol^{-1}) at 300 K. While there are some deviations in the detail, the simulations give an overall good description of the experimental data. These rates were used to calculate the whole T_1 dependence (solid line in Fig. 7).

Comparing the values of the quadrupolar coupling constant obtained from the line shape analysis with the $K^{EFG} = 0.3\pi^2$ (60 kHz)^2 value from the relaxation data it is evident that K^{EFG} is in between the values expected for rotational diffusion and jump diffusion, which can be considered as the limiting cases of the motions responsible for the relaxation. Assuming that the T_1 relaxation is not the effect of another motional process it follows that in our system the motional process responsible for the relaxation is somewhere in between a pure two site jump [eqn. (12c)] and a free rotational diffusion [eqn. 12(b),(d)]. Possible mechanisms for such a relaxation could be a combination of torsional vibrations with the jump process, which would account for larger changes in the quadrupolar interaction and thus faster relaxation or some fourfold distortions of the simple twofold potential of eqn. (1), which might lead to the existence of additional minima at angles of 0 and 180°, which, while not contributing to the spectra might contribute to the T_1 relaxation data.

Another possible reason for the difference could be in the quantum mechanical nature of the D_2 system itself. The relaxation rates given in eqn. (12) are calculated for single particle interactions. However the two deuterons act as a quantum mechanical system of identical particles. It has been shown experimentally and theoretically that *para-* and *ortho*-dideuterium have different spin lattice relaxation rates.[44,45] A similar effect could also be true for the *para* and *ortho* states of the η^2 bound Ru–D_2.

A final answer to this problem can only be given if more experimental relaxation data are available, which are not easy to obtain due to the low sensitivity of the sample.

Summary and conclusion

In summary the ^{2}H NMR spectra and spin lattice relaxation rates of a selectively labeled RuD_2 complex have been measured. The spectra have been analyzed employing a model of a combination of coherent and incoherent exchange processes, described by temperature dependent coherent exchange rates X_{12} and incoherent exchange rates k_{12}. To the best of our knowledge this is for the first time that coherent rotational tunneling has been observed in a solid dideuteride complex by NMR spectroscopy.

From the rates X_{12}, which manifest themselves as the tunnel splitting between the lowest even and odd wave functions, the depth of the rotational potential has been estimated to be 270 meV (6.22 kcal mol^{-1}). This value is in good agreement ,with the height of the tunnel barrier obtained with a Bell tunnel model from the incoherent exchange rates at low temperature (262 meV, 6.03 kcal mol^{-1}). While the coherent rate exhibits only a weak temperature dependence, the incoherent rate grows quickly as the temperature increases. This fast growth is an indication that the one-dimensional model of eqn. (1) is not sufficient to describe the whole dynamics in the system, due to possible changes in the R_{HH} and therefore also in the R_{RuH} distances, which need to be described in a two- or three-dimensional tunnel model. As a simple approximation of such a multi-dimensional tunnel model we have introduced a simple temperature dependent effective barrier height into the Bell tunnel model. Using this model a good description of the whole temperature dependence of the incoherent rate is found. A more detailed analysis of our data could be done by quantum chemical calculations on a level which is beyond the scope of this paper and should be performed by a group of theoretical quantum chemists. Moreover our data, together with the conceptual simplicity of our approach of interpretation, employing Alexander–Binsch theory and a modified one-dimensional tunneling, could help in the understanding of more complex systems, like $-CD_3$ or ND_4.

Finally, we would like to note that the direct visibility of quantum mechanical exchange processes in ^{2}H solid state NMR spectra is not restricted to transition metal complexes, but should be expected in any system with a suitable rotational barrier for the deuterium exchange, for example $-ND_2$ groups, frozen D_2O, *etc.* Thus it would be worthwhile to investigate such systems at low temperatures.

Acknowledgements

RHM thanks NSERC Canada for an operating grant, Nick Plavac for help with the solution NMR studies and Prof. Peter MacDonald for preliminary solid state ^{2}H NMR spectra. Financial support of the Deutsche Forschungsgemeinschaft, Schwerpunktsprogramm "Zeitabhängige Phänomene und Methoden in Quantensystemen in der Physik und Chemie", is gratefully acknowledged.

References

1 G. J. Kubas, *Acc. Chem. Res*., 1988, **21**, 120.
2 G. J. Kubas, R. R. Ryan, B. I. Swanson, P. J. Vergamini and H. J. Wasserman, *J. Am. Chem. Soc*., 1984, **116**, 451.
3 P. G. Jessop and R. H. Morris, *Coord. Chem. Rev*., 1992, **121**, 155.
4 D. M. Heinekey and W. J. Oldham, *J. Chem. Rev*., 1993, **93**, 913.
5 S. Sabo-Etienne and B. Chaudret, *Chem. Rev*., 1998, **98**, 2077.
6 T. A. Luther and D. M. Heinekey, *Inorg. Chem*., 1998, **37**, 127.
7 A. Toupadakis, G. J. Kubas, W. A. King, L. B. Scott and J. Huhmann-Vincent, *Organometallics*, 1998, **17**, 5315.
8 P. A. Maltby, M. Steinbeck, A. J. Lough, R. H. Morris, W. T. Klooster, T. F. Koetzle and R. C. Srivastava, *J. Am. Chem. Soc*., 1996, **118**, 5396.
9 S. Gründemann, H.-H. Limbach, G. Buntkowsky, S. Sabo-Etienne and B. Chaudret, *J. Phys. Chem. A*, 1999, **103**, 4752.
10 H. H. Limbach, G. Scherer and M. Maurer, *Angew. Chem*., 1992, **104**, 1414.
11 H. H. Limbach, G. Scherer, M. Maurer and B. Chaudret, *Angew. Chem., Int. Ed. Engl*., 1990, **31**, 1369.
12 H.-H. Limbach, G. Scherer, L. Meschede, F. Aguilar-Parrilla, B. Wehrle, J. Braun, C. Hoelger, H. Benedict, G. Buntkowsky, E. P. Fehlhammer, J. Elguero, J. A. S. Smith and B. Chaudret, *Ultrafast Reaction Dynamics and Solvent Effects, Experimental and Theoretical Aspects*, ed. Y. Gauduel and R. J. Rossky, American Institute of Physics, Woodbury, NY, 1993.
13 J. Eckert and G. J. Kubas, *J. Phys. Chem*., 1993, **97**, 2378.
14 H.-H. Limbach, S. Ulrich, S. Gründemann, G. Buntkowsky, S. Sabo-Etienne, B. Chaudret, G. J. Kubas and J. Eckert, *J. Am. Chem. Soc*., 1998, **120**, 7929.
15 T. Arliguie, B. Chaudret, J. Devillers and R. Poilblanc, *C. R. Acad. Sci., Ser. I*, 1987, **305**, 1523.
16 D. M. Heinekey, N. G. Payne and G. K. Schulte, *J. Am. Chem. Soc*., 1988, **110**, 2303.
17 D. M. Heinekey, J. M. Millar, T. F. Koetzle, N. G. Payne and K. W. Zilm, *J. Am. Chem. Soc*., 1990, **112**, 909.
18 K. W. Zilm, D. M. Heinekey, J. M. Millar, N. G. Payne and P. Demou, *J. Am. Chem. Soc*., 1989, **111**, 3088.
19 D. Jones, J. A. Labinger and J. Weitekamp, *J. Am. Chem. Soc*., 1989, **111**, 3087.
20 S. J. Inati and K. W. Zilm, *Phys. Rev. Lett*., 1992, **68**, 3273.
21 H. H. Limbach, G. Scherer, L. Meschede, F. Aguilar-Parrilla, B. Wehrle, J. Braun, C. Hoelger, H. Benedict, G. Buntkowsky, W. P. Fehlhammer, J. Elguero, J. A. S. Smith and B. Chaudret, *Ultrafast Reaction Dynamics and Solvent Effects, Experimental and Theoretical Aspects*, ed. Y. Gauduel and P. J. Rossky, American Institute of Physics, Woodbury, NY, 1993, p. 225.
22 G. Buntkowsky, H.-H. Limbach, F. Wehrmann, I. Sack, H. M. Vieth and R. H. Morris, *J. Phys. Chem. A*, 1997, **101**, 4679.
23 H. W. Spiess, *NMR Basic Principles and Progress*, ed. P. Diehl, E. Fluck and R. Kosfeld, Springer Verlag, Berlin, 1978, vol. 15, p. 58.
24 K. Schmidt-Rohr and H. W. Spiess, *Multidimensional Solid State NMR and Polymers*, Academic Press, London, 1994.
25 Z. T. Lalowicz, U. Werner and W. Müller-Warmuth, *Z. Naturforsch. A*, 1988, **43**, 219.
26 E. Roessler, M. Taupitz and H. M. Vieth, *Ber. Bunsen-Ges. Phys. Chem*., 1989, **93**, 1241.
27 T. Bernhard and U. Haeberlen, *Chem. Phys. Lett*., 1991, **186**, 307.
28 A. Detken, P. Focke, H. Zimmermann, U. Haeberlen, Z. Olejniczak and Z. T. Lalowicz, *Z. Naturforsch. A*, 1995, **50**, 95.
29 A. Detken and H. Zimmermann, *J. Chem. Phys*., 1998, **108**, 5845.
30 M. Prager and A. Heidemann, *Rotational Tunneling and Neutron Spectroscopy: A Compilation*, available from the authors, 1995.
31 B. Chin, A. J. Lough, R. H. Morris, C. T. Schweitzer and C. D'Agostino, *Inorg. Chem*., 1994, **33**, 6278.
32 C. Scheurer, R. Wiedenbruch, R. Meyer, R. R. Ernst and D. M. Heinekey, *J. Chem. Phys*., 1997, **106**, 1.
33 S. Alexander, *J. Chem. Phys*., 1962, **37**, 971.
34 G. Binsch, *J. Am. Chem. Soc*., 1969, **91**, 1304.
35 D. A. Kleier and G. Binsch, *J. Magn. Reson*., 1970, **3**, 146.
36 S. Szymanski, *J. Chem. Phys*., 1996, **104**, 8216.
37 S. Szymanski, *Annu. Rep. NMR Spectrosc*., 1998, **35**, 794.
38 C. Scheurer, *Theoretical Investigation of Quantum Exchange in Transition Metal Hydrides*, ed. C. Scheurer, ETH Zürich, Zürich, 1998.
39 S. Benz and U. Haeberlen, *J. Magn. Reson*., 1986, **66**, 125.
40 A. Heuer and U. Haeberlen, *J. Chem. Phys*., 1991, **95**, 4201.
41 A. Abragam, *Principles of Nuclear Magnetism*, Clarendon Press, Oxford, 1961.
42 G. Buntkowsky, M. Taupitz, E. Roessler and H. M. Vieth, *J. Phys. Chem. A*, 1997, **101**, 67.
43 B. Chin, A. J. Lough, R. H. Morris, C. T. Schweitzer and C. D'Agostino, *Inorg. Chem*., 1994, **33**, 6278.
44 L. C. ter Beek and E. E. Burnell, *Bull. Magn. Reson*., 1993, **15**, 175.
45 L. C. ter Beek and E. E. Burnell, *Phys. Rev. B*, 1994, **50**, 9245.

Paper 9/04155I